Impact of El Niño onset timing on the Indian Ocean: Pacific coupling and subsequent El Niño evolution

K. P. Sooraj · Jong-Seong Kug · Tim Li · In-Sik Kang

Abstract A relation between the timing of the El Niño onset and its subsequent evolution is examined by emphasizing its association with the Indian Ocean (IO) SST variation. Two types of El Niño events based on the timing of their onset are classified and their characteristics are examined and compared. In general, spring onset (SP) events grow greater in magnitude and their evolutions have a faster transition. On the contrary, summer onset (SU) events are relatively weaker in magnitude and have a slower transition. Moreover, in contrast to the SU events, the SP events have a strong tendency for accompanying an IO dipole and basin-wide type of warming pattern in the El Niño developing and mature phases, respectively. It is demonstrated here that the distinctive evolutions in transition phase of the two events are resulted from the difference in IO SST. The warm IO SST in the SP El Niño event, lead

K. P. Sooraj
Climate Environment System Research Center,
Seoul National University,
Seoul, Korea

J.-S. Kug (✉)
School of Ocean and Earth Sciences and Technology,
University of Hawaii,
Manoa, 2525 Correa Road, HIG 350,
Honolulu 96822, USA
e-mail: kug@hawaii.edu

T. Li
International Pacific Research Center, SOEST,
University of Hawaii,
Honolulu, USA

I.-S. Kang
School of Earth and Environment Sciences,
Seoul National University,
Seoul, Korea

an anomalous easterlies over the western Pacific, which forces a fast termination of El Niño events.

1 Introduction

A great deal of scientific research has been conducted to gain a better understanding of an El Niño onset, its subsequent evolution, and underlying dynamics. It is widely known about the phase locking of ENSO events to the seasonal cycle, as expressed by their tendency to peak towards the end of the calendar year (Rasumusson and Carpenter 1982). El Niño events also exhibit irregularities in the timing of onset, in the amplitude of sea surface temperature (SST) anomalies and in the duration of events (e.g., Neelin et al. 2000).

Several studies have focused on the timing of El Niño onset and its source of irregularity. Some sources of this irregularity shown in previous studies are deterministic chaos associated with the nonlinear dynamics of ENSO (e.g., Jin et al. 1994), changes in the background states (e.g., Wang 1995), an atmospheric forcing due to other climate phenomena such as Monsoon (e.g., Xu and Chan 2001), stochastic weather noise forcing (e.g., Blanke et al. 1997), an atmospheric forcing due to an intraseasonal oscillation in the tropical Pacific (e.g., McPhaden 1999) and seasonally varying strength of ocean-atmosphere coupling in the equatorial Pacific (Horii and Hanawa 2004).

So far, several studies categorized past El Niño events into several categories (Fu et al. 1986; Enfield and Cid 1991). Based on the timing of El Niño onset, the events can be classified into two types: spring (SP) type and summer (SU) type (Xu and Chan 2001). Previous studies (e.g., Neelin et al. 2000; Xu and Chan 2001; Horii and Hanawa 2004) strongly suggested that the evolution of El Niño

events differs considerably depending on the timing of onset. Neelin et al. (2000), based on their modeling and observational study, suggested that the observed scatter of onset and termination phases is a fundamental ENSO property. Then, Xu and Chan (2001) observed that evolution of the two types of events (SP and SU) is different, but their study did not consider the mechanisms for the difference in evolution of the two events. Recently, Horii and Hanawa (2004) addressed this issue and they mainly attributed this difference to the seasonally varying strength of the ocean-atmosphere coupling (i.e., magnitude of air-sea couple instability) in the equatorial Pacific (Tziperman et al. 1998). We believe that this kind of classification is important to elucidate the El Niño dynamics.

On one hand, there were a number of studies aimed on the impact of ENSO in the Indian Ocean (IO) (e.g., Klein et al. 1999; Reason et al. 2000; Venzke et al. 2000; Xie et al. 2002; Lau and Nath 2003; Li et al. 2003; many others). According to them, IO SST variability is mostly affected by modulation of walker circulation associated with ENSO. On the other hand, there is a recent increase in research interest on the possible role of IO variability on ENSO variability and several scientists have paid special attention to study this aspect in detail (e.g., Yu et al. 2002; Wu and Kirtman 2004; Kug et al. 2005; Kug and Kang 2006; and Kug et al. 2006a,b; Dommenget et al. 2006). In particular, Kug and Kang (2006) emphasized the importance of interactive feedback between ENSO and the IO on fast transition of El Niño events.

This study focuses on the two types of El Niño events (SP and SU) by considering co-variability over the IO. It is known that the evolution of the El Niño events changes considerably with their timing of onset. Hence, it would be of interest to examine how the IO interactive feedback, suggested by Kug and Kang (2006), operates in the evolution of these two events. Therefore, we here explore the relationship between the timing of El Niño onset and the IO-El Niño coupling and we also examine the factors that lead to this coupling and feedback. We further see how this feedback leads to different aspects in their subsequent evolution, using observational data.

The data and classification of the El Niño events based on their onset timing are described in Sect. 2. The spatial and temporal evolutions of the two events are documented in Sect. 3.1 Section 3.2 examines the initiation and development of IO variability during the El Niño developing period. Section 3.3 shows the transition characteristics of each type of events and it examines the IO feedback mechanism in each event. It further describes the dynamical coupling process between ENSO and IO in each type of event. Finally, we discuss the results and their implications in Sect. 4.

2 Data and classification of El Niño events

The data utilized are monthly means of SST, atmospheric circulation data, and ocean temperature for the period of 1958–2000. Anomalies presented in this study were detrended after removing monthly climatology. Atmospheric circulation data were taken from National Center for Environmental Prediction/National Centre for Atmospheric Research (NCEP/NCAR, Kalney et al. 1996), which has a horizontal resolution of 2.5° Lon. x 2.5° Lat. The SST data are from the improved extended reconstructed sea surface temperature version 2 (ERSST.v2) data set (Smith and Reynolds 2004) created by the National Climate Data Center (NCDC). Ocean temperature data were obtained from the Simple Ocean Data Assimilation (SODA) product (Carton et al. 2000a,b). It is available at 0.45° latitude x 1° longitude resolution in the Tropics and has 20 vertical levels with 15-m resolutions near the sea surface. Xie et al. (2002) showed that the SODA data have a good agreement with the expendable bathythermograph (XBT).

We define an El Niño event, using the 5-month running mean of Nino 3.4 index (SST Anomalies, SSTA, averaged over the region 5°S–5°N, 170°W–120°W). El Niño events are defined when Nino 3.4 index exceeds 0.5°C and persisted there afterwards for at least 6 months. The month when the Nino 3.4 index exceeds 0.5°C is defined as the onset month. We further defined SP and SU type events as the El Niño onsets occurring in spring (March, April, or May) and summer (June, July, and August) seasons, respectively. During the 43-year period of 1958–2000, 12 El Niño events are detected based on our definition. Among these events, we identified five SP and four SU types of events. The 1994/95 El Niño events are excluded because of its short period (cf. Kang et al. 2004). Also, we omitted 1977/78 and 1987/88 events, since they are an extension of the previous year warm state. These classifications are similar to those made in earlier studies (Xu and Chan 2001; Horii and Hanawa 2004), but with slight modifications. Thus the SP type events include the years 1965/66, 1972/73, 1982/83, 1991/92, and 1997/98. And the other, SU type events contain the years 1963/64, 1968/69, 1976/77, and 1986/87. In order to provide further robustness in the classification, we examined another SSTA index, NINO3, in the same way to identify the timing of El Niño onset. A comparison of the timing of occurrence identified with the NINO3 SST suggests that the classification is essentially the same.

To compare the characteristics of two types of El Niño events, composite analysis was carried out for the two types of El Niño events. The composites are made for those events that occurred during the period (1958–2000), in which both SST and atmospheric circulation datasets are available. The composites are subjected to the standard *t*-

test for statistical significance and only when at the 90% significant levels are retained in the plots. It is found that the above classification can represent significantly different characteristics in the subsequent evolution of each type El Niño event, which will be described and discussed in the following sections.

3 Observational analysis

3.1 Contrasting evolution of two events over the tropical Indian and Pacific domain

Figure 1 shows the time evolution of normalized NINO3.4 SSTA for the SP and SU type of events occurred over the 43-year period (1958–2000). This clearly reveals that the basic characteristics of two types of SP and SU El Niño events are significantly different, as shown in Fig. 1. It is seen that in the SP type of events, NINO3.4 SSTA has a large peak value at the mature phase and they are characterized by relatively regular and faster transition. Further, the SP-type events have a strong biennial tendency in their evolutions from onset to transition phase. In contrast to these features, the SU-type events have smaller SSTA amplitudes in its mature phase and have rather irregular transition with its slow evolutions. In fact, some of the SU events (1968/69, 1976/77, and 1986/87) persist into the next year after the mature phase and so the biennial tendency is not apparent here. This difference is consistent with previous studies (Xu and Chan 2001; Horii and Hanawa 2004). Since the decay of the two types of events is observed to be quite different, it is expected that the physical mechanisms responsible for their phase transition are different. We will show here the difference in
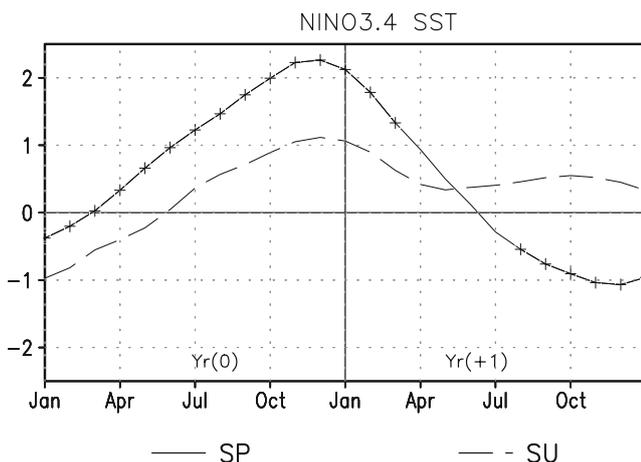

Fig. 1 Time series of normalized Nino-3.4 SSTA for the composite evolution of the SP and SU types of events during the 43-year period (1958–2000). The *cross marks* indicate that the difference between SP and SU composites is significant at 90% confidence level

interaction of the two types of events with the tropical IO and then we will further demonstrate how this interaction contributes to their contrasting evolution by pointing out the possible mechanisms.

Horizontal distribution of SSTA and the related 925-hPa wind anomalies for the SP and SU composites are shown in Figs. 2 and 3, respectively. In the case of the SP composite, warm SSTA begin to appear over the central Pacific and western IO during boreal spring and large SSTA are already established during boreal summer time (Fig. 2a and b). These warm anomalies are accompanied by the anomalous westerlies in the western-central Pacific (Fig. 3a). Noted here that a cyclonic wind flow is appeared over the western north Pacific (WNP), indicating strong WNP monsoon. Also, there is a significant anomalous south-easterly over the eastern IO, indicating that there is an interaction between Pacific and IO variability. Detailed dynamical processes will be discussed in the next subsection.

During the boreal autumn time (Figs. 2c and 3c), anomalous warm SST and westerlies have further developed over the tropical Pacific by the positive ocean-atmosphere feedback process, as firstly suggested by Bjerknes (1969). There are explosive developments of SST and surface wind over the IO as well. Zonal contrast pattern of SST, the so-called IO dipole (IOD) mode suggested by Saji et al. (1999) and Webster et al. (1999), is established now and significant easterly wind is dominant over the IO. Also, there are two distinctive wind systems that are cyclonic flow over the WNP and anticyclonic flow over south eastern IO.

During the boreal winter time (Figs. 2d and 3d), the eastern Pacific SST has reached its maximum phase while over the eastern IO the cold SST has decayed rapidly. The warm SSTA have extended eastward in the IO, resulting in basin-wide warming (BW) over the IO. Also, it seems here that the stronger anomalous winds have moved further eastward compared to its previous season. The southern IO anticyclone has weakened while the WNP cyclonic flow is dramatically changed to an anticyclone. Therefore, the wind anomaly is rapidly changed from westerlies to easterlies. Previous studies pointed out that these abrupt changes are related to the IO SST (Watanabe and Jin 2002; Annamalai et al. 2005; Kug and Kang 2006). In particular, Kug and Kang (2006) further pointed out that the western Pacific (WP) wind changes lead a fast transition from El Niño to La Niña, by generating upwelling Kelvin waves. Consistent with their argument, the SP type of El Niño events represents rapid transition, so that the La Niña is developed in the following year (Fig. 2e).

Unlike the SP composite case, in the SU composite the cold SSTA are still persisting in the central Pacific Ocean (Fig. 2a) during boreal spring time and warm SSTA are not yet fully developed by the El Niño developing summer

Fig. 2 Composites of SSTA for SP (*left*) and SU (*right*) type of events. *Shading* represents the SSTA at 90% confidence level
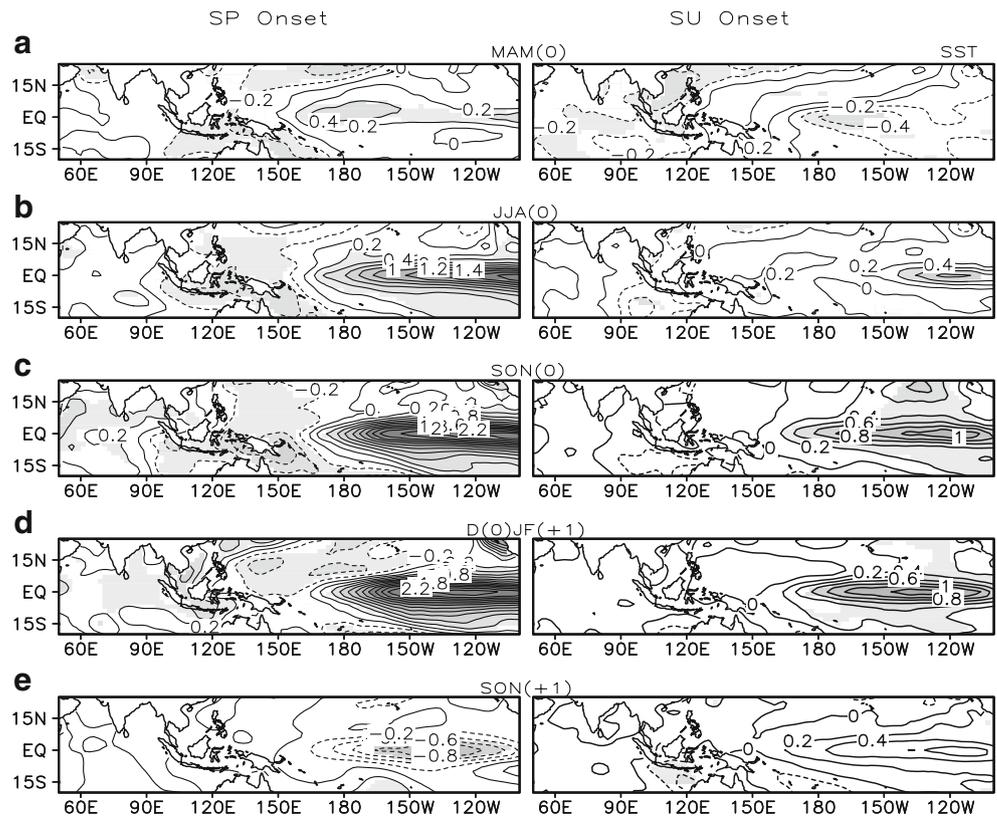

Fig. 3 Composites of 925-hPa Wind anomalies for SP (*left*) and SU (*right*) type of events. *Thick arrows* indicate significant wind vectors at 90% confidence level
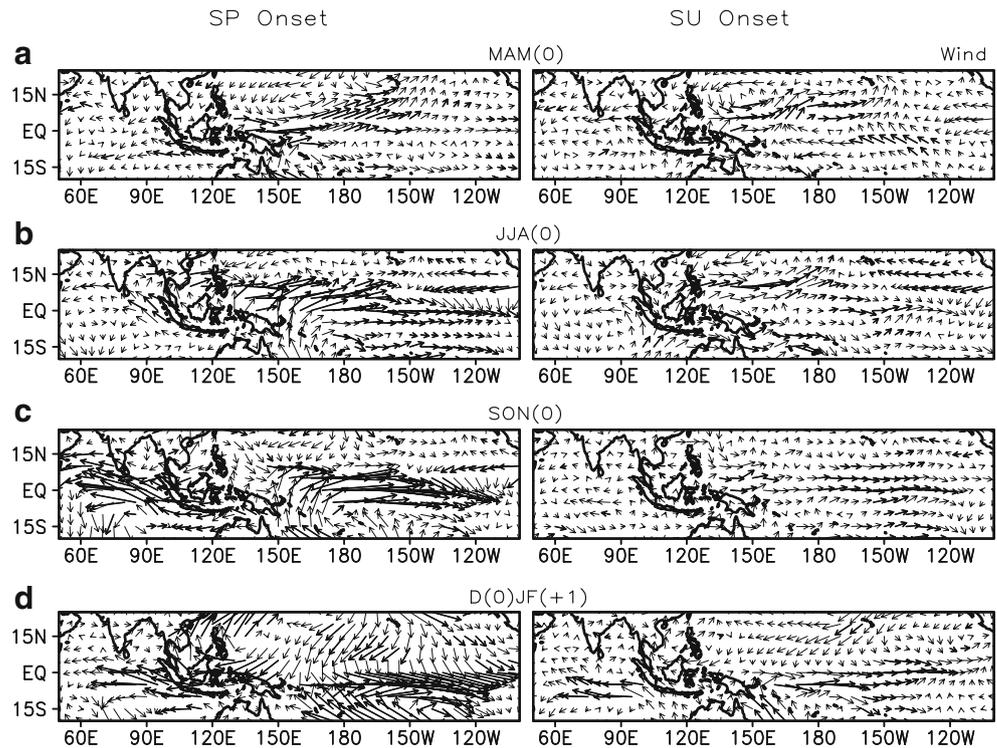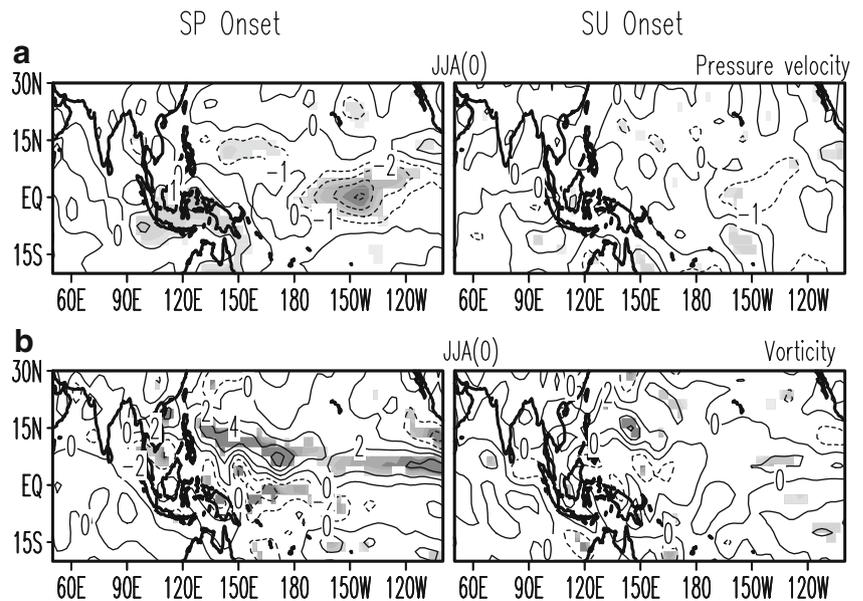
Fig. 4 Composites of 500-hPa pressure velocity anomalies (upper panel, 10^{-2} Pas^{-1}) and 850-hPa vorticity anomalies (lower panel, 10^{-6} s^{-1}) for SP (*left*) and SU (*right*) type of events. *Shading* represents the 90% confidence level

period (Fig. 2b). Therefore, the wind anomalies in the western-central Pacific are relatively weak and the cyclonic flow over the WNP is also weak during boreal summer and fall time. A striking difference from the SU composite is found in the IO (Figs. 2 and 3). There are no significant SST and wind anomalies in the SU composites, while the strong IOD-like pattern is distinctive in the SP composites. During the boreal winter time (Fig. 3d), the wind pattern in the SU composite shows anomalous easterlies in the equatorial IO and anomalous northeasterlies in the north-western Pacific, similar to that of the SP composite, but weaker in magnitude. We also found that anomalous westerlies in the central-eastern Pacific are relatively week. Also no significant anomalous easterlies are found over the WP. Further, in contrast to the SP events, warm SSTA are still persisting in the eastern Pacific in the following autumn season (Fig. 2e).

3.2 Mechanism for the initiation and development of IO variability during El Niño developing period

In the previous section, we showed that there is a distinctive difference between the SP and SU events over the IO. The SP events have a more tendency to accompany IOD-type of events than the SU events. We will examine here how the SP El Niño events can lead to this co-variability over the IO, in contrast to SU El Niño events.

As shown in the previous section, the SP events have already attained large SSTAs during the El Niño developing summer, while the SSTA in the SU composite are not yet established. During this period (see Fig. 2b), the warm tropical Pacific SSTA in the SP events modulates the Walker circulation through enhancing convection in central Pacific (Figs. 4a and b) and suppressing convection

in the maritime continent. It is also shown (in Sect. 3.1) that during the El Niño developing summer, an anomalous cyclonic flow appears over the WNP, indicating that the WNP monsoon is strengthened. The strong WNP monsoon during El Niño developing period is also reported from previous studies (Li et al. 2002, 2003, denoted here after by L02; Wang et al. 2003). This cyclonic circulation is induced by the SST warming in the tropical region, as a Gill-type response (Gill 1980) to the central Pacific convective heat source. Figure 4 shows clearly a strong cyclonic flow over the WNP, west of the convective heat source. Therefore, the WNP monsoon is observed to be stronger in the SP events. It should also be noted here that the southern hemispheric cyclonic circulation is weaker compared to its northern counterpart, making it asymmetric response rather than symmetric response to the heat source, possibly due to the effect of the mean vertical easterly shear associated with Monsoon flow (Wang and Xie 1996; Xie and Wang 1996).

How is the tropical Pacific variability linked to the IO variability in the SP El Niño events? Since the positive air–sea coupled process is active during boreal summer and autumn seasons, the IO variability is easily amplified if any external forcing is given to the IO. There are two possible mechanisms by which the El Niño SST can kick off the IO variability. Firstly, the sinking motion over the Maritime continent (see Fig. 4a) can play a role in inducing the IO variability. Because the sinking motion accompanies low-level divergence (Fig. 3b), there are anomalous surface easterlies over the eastern IO. In the SP composite, anomalous easterly is developed during boreal summer of El Niño developing year. Once the easterly wind is developed over the IO during summer time when the air-sea coupling is strong, the IOD-like SST pattern and wind anomalies are further developed, as suggested by previous

studies (Saji et al. 1999; Webster et al. 1999). Figure 5a shows the composite evolution of the zonal wind anomaly area-averaged over east IO region (80–100°E, and 5°S-5°N). It is clear that in the SP composite, the zonal wind anomaly starts to develop from the early summer and then rapidly intensifying (in contrast to the SU composite), indicating that the local IO air-sea coupled process as well as the external forcing are actively associated with El Niño. The zonal wind anomaly reaches its maximum during October to November and the anomalous easterlies decays rapidly there afterwards, with the abrupt demise of the eastern IO cold SSTA, while the Pacific SST is still developing.

Secondly, the El Niño SST can affect the IO variability through the interaction between the WNP monsoon and IOD. The strong WNP monsoon can trigger IOD variabil-
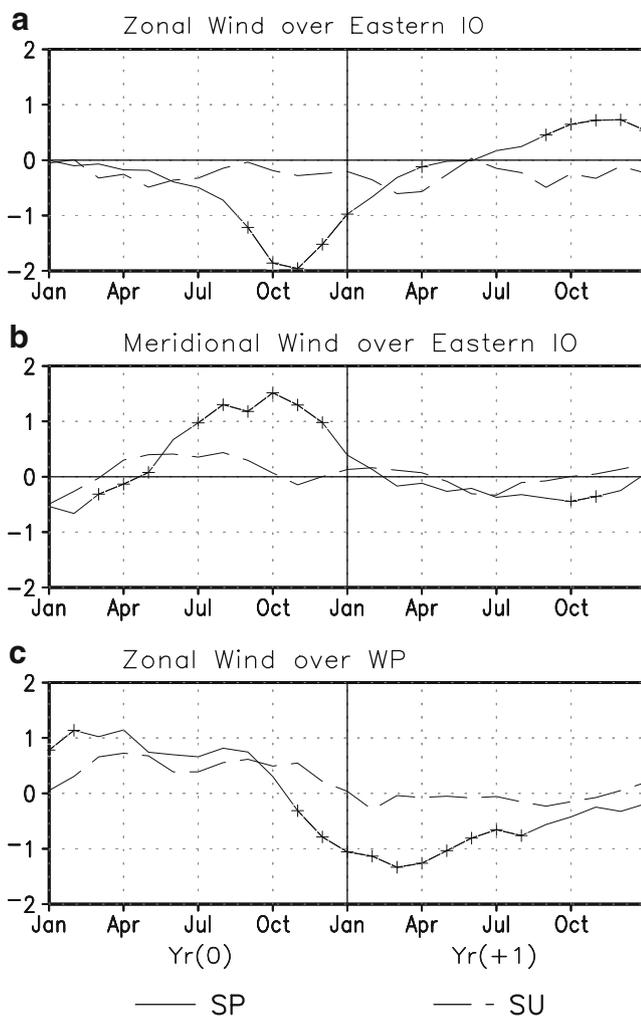

Fig. 5 **a** Composite time evolution (normalized index) of 925-hPa zonal wind anomalies averaged over east IO (80–100E, 5S-5N) for the period 1958–2000. In **b**, same as (**a**), but for meridional Wind over east IO. In **c**, same as (**a**), but for zonal wind averaged over WP (130–150E, 5S- 5N). The *cross marks* indicate that the difference between SP and SU composites is significant at 90% confidence level

ity. The effect of WNP monsoon on IOD was first pointed out by L02. According to them, the enhanced WNP convection can induce cross-equatorial southerlies in the east IO by the Rossby wave response to the off-equatorial heating. On the acceleration of southeasterlies over the southeastern IO, Kajikawa et al. (2003) suggested that it is closely linked to the meridionally asymmetric anomalous convection between the South China/Philippine Sea and the south of the maritime continent, during boreal summer. According to them, these meridionally asymmetric convective anomalies during boreal summer are caused by an anomalous Hadley cell over the WP (between maritime continent and South China/Philippine Sea), which enhances the southeast trade winds over the southeastern equatorial IO. Recently, Huang and Shukla (2007) have shown more evidences to this through coupled model experiments. They found that in the absence of ENSO cycle, the IOD can still be triggered by the fluctuation of the WNP monsoon through this anomalous Hadley cell over the WP.

Figure 5b shows meridional wind anomalies (averaged over the east IO region). During the El Niño developing summer, there is a robust cross equatorial wind anomaly, in contrast to the smaller zonal wind anomaly (see Fig. 5a,b). Noted here that the magnitude of the meridional wind in the SP composite is twice, compared to that in the SU composite. These anomalous southeasterlies increase total wind speed because the climatological wind is also southeasterlies. The increasing wind speed leads more latent heat flux and induces anomalous SST cooling over the eastern IO. Once cold SSTA is developed, these anomalies are further enhanced by the local air-sea feedback as we pointed out before. In the SU events, the SSTA is not so much developed during the El Niño developing summer season that it weakly affects the WNP monsoon. Hence it hardly triggers the IO air-sea coupled feedback. Therefore, the SU El Niño events have no significant variability over the IO, as shown in Figs. 2 and 3.

We again examined the relationship between the WNP monsoon and cross equatorial flow in the east IO by regressing the WNP shear index (derived by following definition of Wang and Fan 1999) on to the 925-hPa wind (both for the JJA season) for the period 1958–2000 (Fig. 6). It shows the stronger southerly flow along the coast of east IO, indicating that the cross equatorial flow is much related to the WNP monsoon activity. The correlation coefficient over the east IO is more than 0.5 with 95% confidence level.

We further analyzed the relationship of the east IO cross equatorial flow with the IO SSTA for the SON period. We found that the cross equatorial flow is strongly related with the cold eastern IO SSTA (averaged over 80–110°E, 10°S-equator) with the correlation coefficient assuming values of -0.60 (significant at more than 99% confidence level).
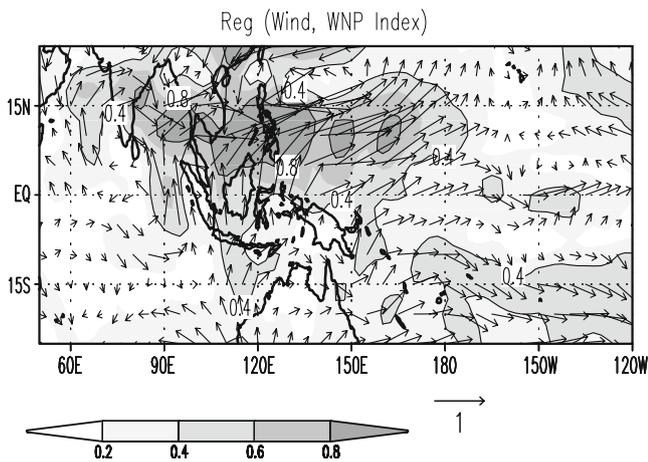
Fig. 6 Regression (*vector arrows*) and correlation (*shading*, represented by the magnitude of wind) of 925-hPa wind with the WNP shear index (derived by following definition of Wang and Fan 1999)

Similarly, the correlation coefficient between the cross equatorial flow and the western IO SSTA (averaged over 55–70°E, 10°S-10°N) is found to be 0.54, which is significant at more than 95% confidence level. Therefore, the dipole mode index (DMI, as defined in Saji et al. 1999) is also found to be strongly correlated (0.7, significant at more than 99% confidence level) with the cross equatorial flow.

The processes shown in the SP events are to a large extent, very similar to the developing mechanism of IOD, for which the external ENSO forcing is necessary for triggering the air–sea coupled feedback over IO (Allan et al. 2001; Lau and Nath 2004). Considering this aspect, we examined the DMI for the two types of El Niño events. The composite DMI is shown in Fig. 7a. It shows stronger warm IOD events (as indicated by positive value of DMI, of about 1.5 standard deviation) in the SP, during the autumn season of the El Niño developing period. In contrast to this, the SU events are marked with low value of DMI during its developing period.

During the summer and autumn of the El Niño developing year, the IO SST plays an active role by inducing anomalous Walker circulation. However, during the spring time of the El Niño decaying year, it seems that the IO SSTA does not play an active role, in spite of the warm SST anomaly over there. This is because there is sinking motion over the IO, which itself can induce the warm SST anomaly through excessive short-wave radiation. This seasonal dependency of the IO feedback needs more detailed work in the future.

3.3 IO feedback and fast transition of El Niño

So far we showed the difference in evolution of two events over the tropical Indian and Pacific domain and the factors that cause IO warming in the two events. In this subsection,

we will examine how this IO warming or the so-called IO feedback affects the transition of the two events (Kug and Kang 2006).

Figure 5c shows the 925-hPa zonal wind averaged over the WP region (130–150°E, 5°S-5°N). The contrasting evolution of anomalous easterlies in the two events is shown in Fig. 5c, with the SP events, compared to the SU, attaining larger magnitudes after the mature phase. Also, in the SP events, there is a sudden transition of WP zonal wind anomaly from positive in the developing autumn period to negative in the mature phase. On the contrary, the SU events are associated with a slow transition of WP zonal wind anomaly. Interestingly, it is to be noted here that this sudden reversal of the zonal wind from westerly to easterly in the SP events is associated with the rapid transition of the IOD type of warming to (see Fig. 7a and b) a uniform BW mode in IO during D(0)JF(+1), when the Pacific ocean SSTA does not change rapidly.

One may ask whether the anomalous WP zonal wind, which leads a faster transition of the SP El Niño composite, results from the IO feedback. Because the magnitude of the SP El Niño events is larger than that of the SU El Niño
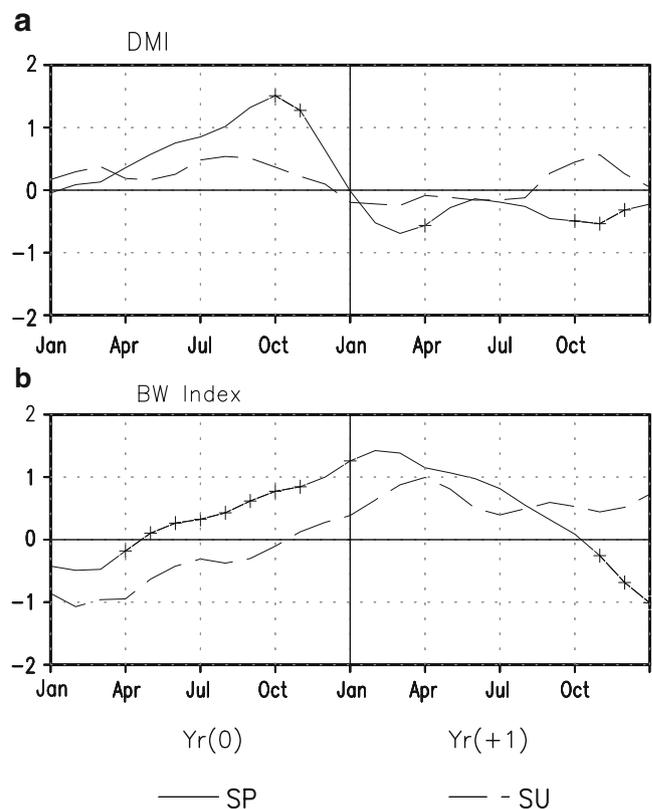

Fig. 7 Composite (for SP and SU) time evolution (normalized index) of **a**. DMI (by following the definition by Saji et al. 1999) and **b** basin wide index (as defined by An 2004). The *cross marks* indicate that the difference between SP and SU composites is significant at 90% confidence level
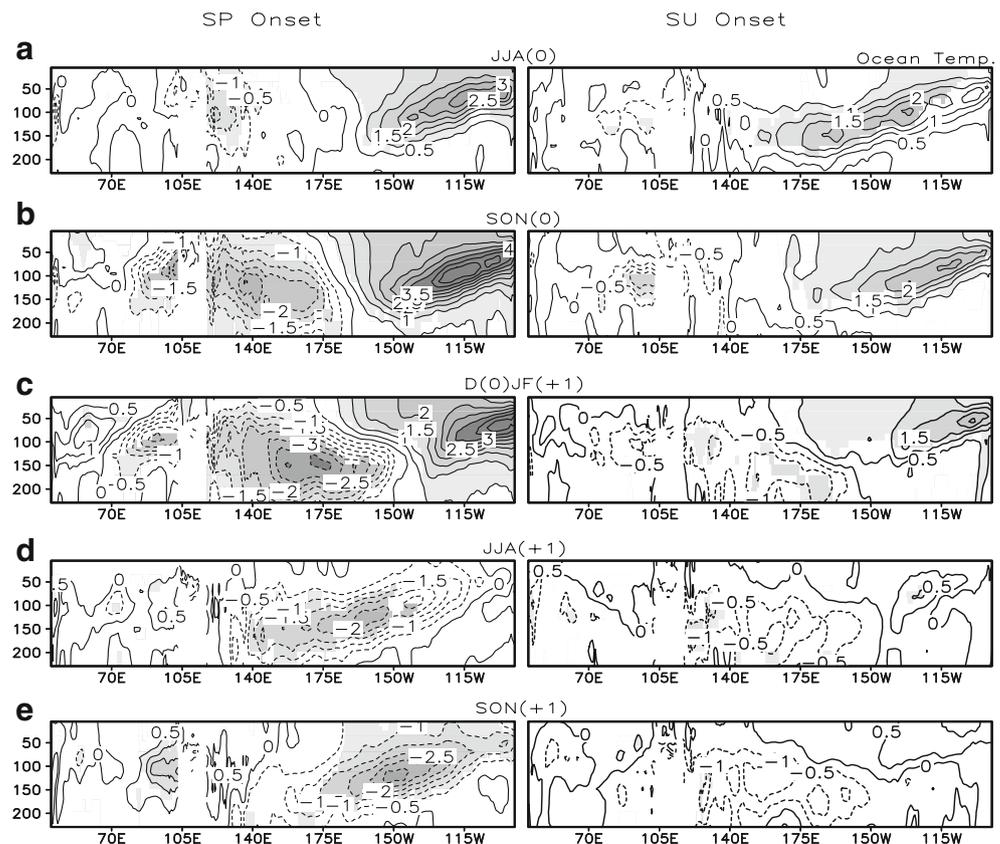
events, this may come from the Pacific SST itself. To check this, we calculated the ratio of the different variables between SP and SU composites during December–January, when the El Niño amplitude is at peak. The ratio for NINO3.4 SST is about 2.5. The ratio for the central-eastern Pacific zonal wind anomalies (averaged over 170–240°E, 5°S-5°N, where anomalous westerlies dominate), is found to be 2.7, which is comparable with that of NINO3.4, indicating that the wind anomalies are directly induced by the tropical SST forcing. However, the ratio for WP zonal wind index is about 9.0. This indicates that with only SST anomaly over central-eastern Pacific one can not fully explain the WP wind variability. Also, this at least means that the difference in magnitudes of two types of El Niño events cannot fully explain the change in the WP winds. So, this implies that the IO SSTA plays some crucial role in developing the WP wind anomalies.

Recently, Annamalai et al. (2005), using atmospheric GCM experiments, and Ohba and Ueda (2007), using air-sea coupled GCM experiments, have shown that the IOD warming does not have a significant impact on tropical Pacific wind variability, while the BW can influence on the tropical Pacific wind variability. According to Ohba and Ueda (2007), the BW during boreal winter enhances the surface easterlies over the equatorial WP, which induces an advanced transition to the La Niña phase.

The role of IO SST warming in affecting the development of the anomalous easterlies in the WP has been well studied by Kug and Kang (2006). They have done atmospheric GCM experiments to reveal the influence of IO SST on the WP wind anomaly by superposing climatological SSTs on seasonally varying SST anomalies. They conducted mainly three sensitivity experiments, by imposing SST anomalies in the global, Pacific (30°S–30°N, 120°E–80°W) and IO (30°S–30°N, 40–120°E), respectively. From these experiments they found that the IO warming is a more effective contributor to developing the anomalous easterlies than the warming in the eastern Pacific. They suggested the role of eastward expansion of anomalous Walker circulations in modulating the WP wind variability. Earlier, Misra (2004) noted that SST anomalies in the western IO are the most effective in influencing the convection over the WP, through their study based on observations and AGCM. According to them, a positive SST anomaly in SON(0) and DJF(+1) seasons over the western IO, increase the contemporaneous positive OLR anomalies over the WP ocean. Our results are also consistent with their study.

Figure 8 shows the evolution of ocean temperature along the equator in the two events. For the SP events, during the development phase of the El Niño, the subsurface temperature is developed overwhelmingly in the eastern Pacific

Fig. 8 Composites of ocean temperature anomalies along equator for SP (*left*) and SU (*right*) type of events. *Shading* represents the ocean temperature with 90% confidence level

(Fig. 8 a,b). Simultaneously, cold temperature anomalies start developing over the WP also, and a drastic change occurs during the El Niño mature phase when this cold temperature in the WP develops explosively (Fig. 8c). This may be attributed to the abrupt establishment of anomalous easterlies in the WP as shown earlier in Figs. 3d and 5c. During the boreal summer of the following year (Fig. 8d), a cold subsurface temperature has developed (see it is statistically significant at 90% confidence level over the central Pacific) over the whole Pacific Basin. This cold subsurface temperature then propagates eastward along the equator and forces the termination of El Niño. The easterlies have further developed over the WP by the positive air–sea coupled feedback (Bjerknes 1969). Once the cold SSTA appear in the central and eastern Pacific, it is further developed by the air–sea coupled process. However, for the SU events, the cold subsurface temperature anomaly is relatively weak in the WP (Fig. 8d), as the anomalous easterly wind is feeble (Fig. 5c). Therefore, El Niño decays slowly since its mature phase. Therefore, it is seen here that the WP wind anomalies significantly affect the structure of the ocean temperature (as shown in Fig. 8) over the whole Pacific Basin. It is due to the reason that these wind anomalies excite oceanic Kelvin waves, thus changing the oceanic vertical structure (Kug and Kang 2006). It is also seen that there are significant differences in the temperature anomalies over the IO as well, implying the changes are not only confined to the surface level. This indicates the role of ocean dynamics in the process contributing to the east-west dipole (Shinoda et al. 2004). In general, the significant differences (between two types of events) in temperature are not only confined to the Pacific region but also over IO, which implies the IO-Pacific coupling. Moreover, the cold WP temperature anomalies, which precede the occurrence of the IOD and IO (BW) warming and the distinction of it in the two types of events (Fig. 8b,c,d), is quite interesting. This leads us to speculate that these WP temperature anomalies could additionally contribute to the termination of the ENSO.

4 Discussion and summary

It is known that the evolution of El Niño event differs considerably depending on the timing of onset. So, we here explore the relationship between the timing of El Niño onset and the IO-El Niño coupling using observational data (for the period 1958–2000). We examined here how this coupling and its feedback leads to different aspects in the subsequent evolution of the two events. We showed the mechanism which generates this IO feedback and its difference in the two contrasting events. Our result suggests that in the SP composite, WNP monsoon plays a role in strengthening the cold SSTA in the east IO and this coupled with local air-sea feedback gives a rise to IO feedback during the El Niño developing summer and autumn. This result is in confirmation with L02, Kajikawa et al. (2003) and Huang and Shukla (2007). Also, in the case of the SP events, there is a sudden transition of WP zonal wind anomaly from positive in the developing autumn period to negative in the mature phase of the El Niño. Further, it is observed to be associated with the transition of the IOD to a uniform BW mode in the IO. These anomalous easterlies excite upwelling Kelvin waves, which rapidly propagate eastward and lead to relatively faster transition of the SP events. This is similar to the mechanism suggested by Kug and Kang (2006). In the case of the SU events, the SSTA is relatively weak during the El Niño developing summer season that it fails to generate this IO feedback mechanism.

We checked the robustness of the proposed coupling process in this study by conducting a similar analysis with less-intense SP events (1965/66, 1972/73, and 1991/92). The results still hold with relatively intense WNP monsoon and the IO feedback. Also, the IO feedback and the subsequent El Niño transition are more evident and stronger than the SU composites, but slightly weaker compared to the earlier SP composites.

We have done a similar study by analyzing the horizontal distribution of SSTA composites for the SP and SU type of events that occurred over the 100-year period (1901–2000). The two-type events (for 1901–2000) are again categorized based on the same definition as described in Sect. 2. Based on this period, we obtained eight SP and eight SU onset events. The composite evolution of both types of events shows a similar type of evolution and transition, with SP events showing faster transition, in contrast to SU. Also, we observed that in contrast to the SU events, the SP events have a strong tendency to accompany IO warming during El Niño developing and mature phase (figure not shown). This suggests that our results are quite robust, regardless of the observational data period. We repeated this analysis by removing decadal-interdecadal variations (periods exceeding 8 years) from the original SSTA data sets and obtained similar results (not shown). Thus, the results seem still valid even without decadal variability.

This study is an extension of the previous study done by Kug and Kang (2006), who classified El Niño events into two groups based on the IO warming. Their study revealed that fast transition of El Niño events is related to the IO feedback. However, they did not answer what dynamical process controls the existence of the IO feedback in many El Niño events. The present study shows that the timing of the onset and WNP monsoon partly contributed to the existence of the IO feedback. In fact, most SP onset events are consistent with their "WISST" events (see Kug and

Kang 2006), which is accompanied by the IO. This study may have useful implication for ENSO prediction. A number of El Niño prediction models cannot consider the sudden transition of WP anomaly associated wind-IO feedback, since they are developed based on the tropical Pacific domain. So it means that they cannot correctly predict a fast transition event such as an SP event. Also, by monitoring the onset time of an ongoing El Niño event, it can be used to predict the changes in tropical Pacific SST in the El Niño evolution stage.

Generally, the predictive skills of the dynamical and statistical model are degraded for El Niño onset period. Hence, the El Niño onset is a challenging problem of ENSO prediction. In the same line, it is unclear what dynamical processes determine the timing of onset, though the sequential evolution of El Niño events highly depends on their onset timing, as the present study reveals. Recently, Kug et al. (2008) found that the activity of fast atmospheric variability over the WP can be used as a precursor for El Niño onset. Their results suggest that stronger activities for the atmospheric noise are observed over the WP about 7–10 months prior to the mature stage of El Niño. In fact, our further analysis with the two events shows stronger (weaker) atmospheric noise activity over the WP in the initial period of onset of SP (SU) events (not shown here). This implies the interaction with the stochastic atmospheric noise is a crucial factor in determining the onset timing. However, further work should be done in this direction.

References

Allan R, Coauthors (2001) Is there an Indian Ocean dipole, and is it independent of the El Niño–Southern Oscillation? CLIVAR Exch 6:18–22

An S-I (2004) A dynamical linkage between the monopole and dipole modes in the tropical Indian Ocean. Theor Appl Climatol 78:195–201

Annamalai H, Xie SP, McCreary JP, Murtugudde R (2005) Impact of Indian Ocean sea surface temperature on developing El Niño. J Climate 18:302–319

Bjerknes J (1969) Atmospheric teleconnections from the equatorial Pacific. Mon Wea Rev 97:163–172

Blanke R, Neelin JD, Gutzler D (1997) Estimating the effect of stochastic wind stress forcing on ENSO irregularity. J Climate 10:1473–1486

Carton JA, Chepurin GA, Cao X, Giese BS (2000a) A simple ocean data assimilation analysis of the global upper ocean 1950–1995, Part I: methodology. J Phys Oceanogr 30:294–309

Carton JA, Chepurin GA, Cao X, Giese BS (2000b) A simple ocean data assimilation analysis of the global upper ocean 1950–1995 Part II: results. J Phys Oceanogr 30:311–326

Dommenget D, Semenov V, Latif M (2006) Impacts of the tropical Indian and Atlantic Oceans on ENSO. Geophys Res Lett 33: L11701. doi:10.1029/2006GL025871

Enfield DB, Cid LS (1991) Low-frequency changes in El Niño-Southern Oscillation. J Climate 4:1137–1146

Fu C, Diaz HF, Fletcher JO (1986) Characteristics of the response of sea surface temperature in the central Pacific associated with warm episodes of the Southern Oscillation. Mon Wea Rev 114:1716–1738

Gill AE (1980) Some simple solutions for heat-induced tropical circulation. QJ R M S 106:447–462

Horii T, Hanawa K (2004) A relationship between timing of El Niño onset and subsequent evolution. Geophys Res Lett 31:L06304. doi:10.1029/2003GL019239

Huang B, Shukla J (2007) Mechanisms for the interannual variability in the tropical Indian Ocean. Part II: regional processes. J Climate 20:2937–2960

Jin F, Neelin D, Ghil M (1994) El Niño on the devil's staircase: annual subharmonic step to chaos. Science 264:70–72

Kajikawa Y, Yasunari T, Kawamura R (2003) The role of the local Hadley circulation over the western Pacific on the zonally asymmetric anomalies over the Indian Ocean. J Meteor Soc Japan 81–2:259–276

Kalney E, Co-authors (1996) The NCEP/NCAR 40-year reanalysis project. Bull Am Meterol Soc 77:437–471

Kang I-S, Kug J-S, An S-I, Jin F-F (2004) A near-annual Pacific Ocean basin mode. J Climate 17:2478–2488

Klein SA, Soden BJ, Lau NG (1999) Remote sea surface temperature variation during ENSO: evidence for a tropical atmosphere bridge. J Climate 12:917–932

Kug J-S, Kang I-S (2006) Interactive feedback between ENSO and the Indian Ocean. J Climate 19:1784–1801

Kug J-S, An S-I, Jin F-F, Kang I-S (2005) Preconditions for El Niño and La Niña onsets and their relation to the Indian Ocean. Geophys Res Lett 32:L05706. doi:10.1029/2004GL021674

Kug J-S, Kirtman BP, Kang I-S (2006a) Interactive feedback between ENSO and the Indian Ocean in an interactive coupled model. J Climate 19:6371–6381

Kug J-S, Li T, An S-I, Kang I-S, Luo J-J, Masson S, Yamagata T (2006b) Role of the ENSO-Indian Ocean coupling on ENSO variability in a coupled GCM. Geophys Res Lett 33:L09710. doi:10.1029/2005GL024916

Kug J-S, Jin F-F, Sooraj KP, Kang I-S (2008) Evidence of the state-dependent atmospheric noise associated with ENSO. Geophys Res Lett. doi:10.1029/2007GL032450

Lau N-C, Nath MJ (2003) Atmosphere-ocean variations in the Indo-Pacific sector during ENSO episodes. J Climate 16:3–20

Lau N-C, Nath MJ (2004) Coupled GCM simulation of atmosphere-ocean variability associated with zonally asymmetric SST changes in the tropical Indian Ocean. J Climate 17:245–265

Li T, Zhang Y, Lu E, Wang D (2002) Relative role of dynamic and thermodynamic processes in the development of the Indian Ocean dipole: an OGCM diagnosis. Geophys Res Lett 29:2110. doi:10.1029/2002GL05789

Li T, Wang B, Chang C-P, Zhang Y (2003) A theory for the Indian Ocean dipole-zonal mode. J Atmos Sci 60:2119–2135

McPhaden MJ (1999) Genesis and evolution of the 1997–1998 El Niño. Science 283:950–954

Misra V (2004) The teleconnection between the western Indian and the western Pacific Oceans. Mon Wea Rev 132:445–455

Neelin JD, Jin F-F, Syu HH (2000) Variations in ENSO phase locking. J Climate 13:2570–2590

Ohba M, Ueda H (2007) An impact of SST anomalies in the Indian Ocean in acceleration of the El Niño to La Niña transition. J Meteor Soc Jpn 85:335–348

Rasumusson EM, Carpenter TH (1982) Variations in tropical sea-surface temperature and surface wind fields associated with the Southern Oscillation El Niño. Mon Wea Rev 110:354–384

Reason CJC, Allan RJ, Lindesay JA, Ansell TJ (2000) ENSO and climate signals across the Indian Ocean basin in the global contest: part I, Interannual composite patterns. Int J Climatol 20:1285–1327

Saji NH, Goswami BN, Vinayachandran PN, Yamagata T (1999) A dipole mode in the tropical Indian Ocean. Nature 401:360–363

Shinoda T, Alexander MA, Hendon HH (2004) Remote response of the Indian Ocean to interannual SST variations in the tropical Pacific. J Climate 17:362–372

Smith TM, Reynolds RW (2004) Improved extended reconstruction of SST (1854–1997). J Climate 17:2466–2477

Tziperman E, Cane MA, Zebiak SE, Xue Y, Blumenthal B (1998) Locking of El Niño peak time to the end of the calendar year in the delayed oscillator picture of ENSO. J Climate 11:2191–2199

Venzke S, Latif M, Villwock A (2000) The coupled GCM ECHO-2. Part II: Indian Ocean response to ENSO. J Climate 13:1371–1383

Wang B (1995) Interdecadal changes in El Niño onset in the last four decades. J Climate 8:267–258

Wang B, Xie X (1996) Low-frequency equatorial waves in vertically shear flow. Part I: stable waves. J Atmos Sci 53:449–467

Wang B, Fan Z (1999) Choice of South Asian Summer Monsoon Indices. Bull Am Meteorol Sci 80:629–638

Wang B, Wu R, Li T (2003) Atmosphere–warm ocean interaction and its impact on Asian-Australian Monsoon variability. J Climate 16:1195–1211

Watanabe M, Jin F-F (2002) Role of Indian Ocean warming in the development of the Philippine Sea anticyclone during ENSO. Geophys Res Lett 29:1478. doi:10.1029/2001GL014318

Webster PJ, Moore AM, Loschnigg JP, Leben RR (1999) The great Indian Ocean warming of 1997–98: evidence of coupled oceanic-atmospheric instabilities. Nature 401:356–360

Wu R, Kirtman BP (2004) Understanding the impacts of the Indian Ocean on ENSO variability in a coupled GCM. J Climate 17:4019–4031

Xie X, Wang B (1996) Low-frequency equatorial waves in vertically sheared zonal flows.) Part II: unstable waves. J Atmos Sci 53:3589–3605

Xie S-P, Annamalai H, Schott F, McCreary JP Jr (2002) Structure and mechanisms of South Indian Ocean climate variability. J Climate 15:864–874

Xu JJ, Chan JCL (2001) The role of the Asian-Australian monsoon system in the onset time of El Niño events. J Climate 14:418–433

Yu J-Y, Mechoso CR, McWilliams JC, Arakawa A (2002) Impacts of the Indian Ocean on the ENSO cycle. Geophys Res Lett 29:1204. doi:10.1029/2001GL014098